

AD-A144 951

AN IMPROVED ANALYTICAL THEORY OF ROSSBY WAVE DRIVEN
EULERIAN AND LAGRANGIAN (U) HAWAII INST OF GEOPHYSICS
HONOLULU I S OH ET AL MAY 84 HIG-84-1

1/1

UNCLASSIFIED

NO0014-82-C-0380

F/G 8/3

NL

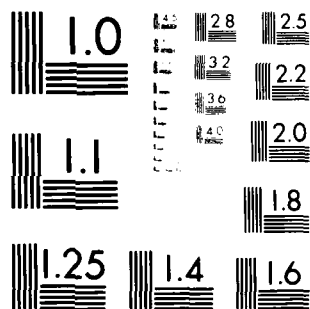
END

DATE

FILMED

9 84

DTIC



MICROCOPY RESOLUTION TEST CHART
NATIONAL BUREAU OF STANDARDS-1963-A

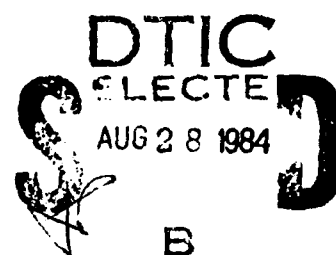
(12)

HIG-84-1

AN IMPROVED ANALYTICAL THEORY OF
ROSSBY WAVE DRIVEN EULERIAN AND LAGRANGIAN MEAN FLOWS
ALONG NON-ZONAL BARRIERS,
WITH APPLICATION TO THE HAWAIIAN RIDGE

IM SANG OH and LORENZ MAGAARD

MAY 1984



DTIC FILE COPY

AD-A144 951

Prepared for
OFFICE OF NAVAL RESEARCH
Contract N00014-82-C-0380

DISTRIBUTION STATEMENT A

Approved for public release
Distribution Unlimited

HAWAII INSTITUTE OF GEOPHYSICS
UNIVERSITY OF HAWAII
HONOLULU, HAWAII 96822



84 08 27 157

HIG-84-1

AN IMPROVED ANALYTICAL THEORY OF
ROSSBY WAVE DRIVEN EULERIAN AND LAGRANGIAN MEAN FLOWS
ALONG NON-ZONAL BARRIERS,
WITH APPLICATION TO THE HAWAIIAN RIDGE

Im Sang Oh
Hawaii Institute of Geophysics

and

Lorenz Magaard
Hawaii Institute of Geophysics
and
Department of Oceanography


University of Hawaii
Honolulu, Hawaii 96822

May 1984

DTIC
ELECTE
AUG 28 1984
B

Prepared for

OFFICE OF NAVAL RESEARCH
Contract N00014-82-C-0380


Charles E. Heisley
Director
Hawaii Institute of Geophysics

DISTRIBUTION STATEMENT A
Approved for public release
Distribution Unlimited

Abstract

We study the reflection of baroclinic Rossby waves from a non-zonal barrier. In doing so we improve and extend an analytical study by Mysak and Magaard (1983). We add lateral friction to their model and obtain not only a more realistic Eulerian secondary flow, but we also calculate the Stokes drift of the total Rossby wave field. We apply our improved and extended model to the Hawaiian Ridge where the incident wave field is known (Magaard, 1983).

Compared to the case of vanishing lateral friction, the Eulerian mean flow now shows smaller current speeds and wider current bands. The narrow eastward jet in the immediate neighborhood of the Ridge is now replaced by a much weaker, broader eastward flow. The subsequent western boundary current and eastward countercurrent are now shifted farther away from the Ridge in better agreement with White's (1983) analysis of historical temperature data. The Lagrangian mean flow is stronger than the Eulerian mean flow. Within the first 100 km off the Ridge the two flows are mostly in opposite directions.

Accession For	
NTIS GRA&I	<input checked="" type="checkbox"/>
DTIC TAB	<input type="checkbox"/>
Unannounced	<input type="checkbox"/>
Justification	
By	
Distribution/	
Availability Codes	
Dist	Avail and/or Special
A-1	



Contents

	Page
Abstract.....	111
List of Figures.....	vii
List of Tables.....	vii
1. INTRODUCTION.....	1
2. THE EULERIAN MEAN FLOW.....	1
3. THE LAGRANGIAN MEAN FLOW.....	8
4. DISCUSSION.....	9
Acknowledgments.....	12
References.....	13

Figures

<u>Figure</u>	<u>Page</u>
1. The horizontal distribution of the surface Eulerian mean flow along the north side of the Hawaiian Ridge.....	7
2. The horizontal distribution of surface mean flows along the north side of the Hawaiian Ridge.....	10

Tables

<u>Table</u>	<u>Page</u>
1. Maximum values of current speed (in ms^{-1}) for the first three bands of the Eulerian mean flow for various combinations of R and A values.....	11
2. \bar{c} - Rossby numbers (\bar{c}) for reflected Rossby waves for various R, A combinations.....	11

1. INTRODUCTION

In a recent paper Mysak and Magaard (1983), henceforth referred to as MM, studied the reflection of baroclinic Rossby waves from a non-zonal barrier. They have shown that the total field of incoming and reflected waves leads to an Eulerian secondary flow, and they applied this theory to the eastern portion of the Hawaiian Ridge area where the incoming Rossby waves are known (Magaard, 1983). The theory predicts an Eulerian mean flow along the Ridge that compares fairly well with a current derived from historical temperature data by White (1983). MM and White called this current the "North Hawaiian Ridge Current."

In their analytical theory MM use Rayleigh damping to reduce the magnitude of the mean flow to realistic values, which necessitates a value of $R = 5 \times 10^{-8} s^{-1}$ for the damping coefficient, i.e. a relaxation time of 200 days. This coefficient cancels out the very low-frequency waves (0.1 to 0.25 cpy range) and still cripples the annual and near-annual waves to such a degree that the whole concept of studying the problem by means of linear reflection theory becomes questionable. Moreover, restriction to Rayleigh damping excludes the possibility of studying the reflection process under a nonslip condition at the barrier, a shortcoming of the MM theory.

In this paper we introduce lateral friction to the study to allow a treatment of the reflection process under a nonslip condition. This introduction allows for smaller values of the Rayleigh damping coefficient, and makes the application of linear wave reflection theory more meaningful.

MM studied only the Eulerian mean flow associated with the incoming and reflected waves. So far there are only Eulerian observations of White to check theories against, and even these observations rest on a very thin data base. In this paper we improve the theory of the Eulerian mean flow generated by the waves, and thus achieve a better agreement between the theory and the Eulerian observations. Moreover, we determine the Lagrangian mean flow by studying the Stokes drift of the waves. A comparison of the theoretically predicted Lagrangian flow with observations must wait until Lagrangian data are available.

2. THE EULERIAN MEAN FLOW

The nondimensional potential vorticity equation with the inclusion of Rayleigh damping and lateral friction reads

$$\frac{D}{Dt} [\nabla^2 \psi + (B^{-1} \psi_z)_z + \beta^* Y] = -R^* \nabla^2 \psi + A^* \nabla^2 (\nabla^2 \psi), \quad (2.1)$$

where X , Y and z are the coordinates in the eastward, northward and upward directions; ψ is the geostrophic pressure; $\nabla^2 = \partial_{XX} + \partial_{YY}$;

$\frac{D}{Dt} = \partial_t - \psi_Y \partial_X + \psi_X \partial_Y$; and B, β^*, R^* and A^* are the nondimensional

parameters:

$$\begin{aligned}
 B &= r_i^2 / \ell^2 \equiv [N^2(z) H^2 / f_0^2] / \ell^2 \quad (\text{Burger number}) \\
 \beta^* &= f_0 \ell^2 \cot \phi_0 / R_e U_0 \quad (\text{planetary vorticity factor}) \quad (2.2) \\
 R^* &= (\ell / U_0) R \quad (\text{nondimensional Raleigh damping parameter}) \\
 A^* &= (\ell U_0)^{-1} A \quad (\text{nondimensional lateral friction parameter}).
 \end{aligned}$$

In (2.2) the dimensional quantities have the following meanings:

$$\begin{aligned}
 r_i &= \text{internal Rossby radius of deformation} \\
 N &= \text{Brunt-Väisälä frequency} \\
 H &= \text{ocean depth} \\
 \ell &= \text{horizontal length scale} \\
 f_0 &= \text{mean Coriolis parameter} \quad (2.3) \\
 \phi_0 &= \text{reference latitude} \\
 U_0 &= \text{horizontal velocity scale} \\
 R_e &= \text{earth's radius} \\
 R &= \text{Rayleigh damping coefficient (of dimension time}^{-1}\text{)} \\
 A &= \text{lateral friction coefficient (of dimension length}^2\text{time}^{-1}\text{)}.
 \end{aligned}$$

Except for the additional lateral friction term (2.1) is the same as (2.1) of MM.

We introduce a set of rotated coordinates x, y which are parallel and perpendicular to the barrier:

$$\begin{aligned}
 x &= X \cos \alpha - Y \sin \alpha \\
 y &= X \sin \alpha + Y \cos \alpha, \quad (2.4)
 \end{aligned}$$

where α is the angle between the barrier and the circles of latitude.

Under the transformation (2.4), (2.1) takes the form

$$\frac{D}{Dt} [\nabla^2 \psi + (B^{-1} \psi_z)_z + \beta^* (-x \sin \alpha + y \cos \alpha)] = -R^* \nabla^2 \psi + A^* \nabla^2 (\nabla^2 \psi), \quad (2.5)$$

where now $\psi = \psi(x, y, z, t)$, $\nabla^2 = \partial_{xx} + \partial_{yy}$ and $\frac{D}{Dt} = \partial_t - \psi_y \partial_x + \psi_x \partial_y$.

In addition to the boundary conditions

$$\psi = 0 \quad \text{at} \quad y = 0 \quad (2.6)$$

and

$$\frac{D}{Dt} \psi_z = 0 \quad \text{at} \quad z = 0, -1 \quad (2.7)$$

we add the nonslip condition

$$\psi_y = 0 \quad \text{at} \quad y = 0. \quad (2.8)$$

The nondimensional velocity components and perturbation density field, ρ , can be computed from ψ via the relations

$$u = -\psi_y, \quad v = \psi_x, \quad w = -\frac{1}{B} \frac{D}{Dt} \psi_z, \quad \rho = -\psi_z. \quad (2.9)$$

Finally, we note that to obtain dimensional quantities (denoted with a superscript d), the following relations must be used:

$$[x^d, y^d, z^d, t^d, u^d, v^d, w^d, p^d, \rho^d] \quad (2.10)$$

$$= [\ell x, \ell y, H z, (\ell/U_0)t, U_0 u, U_0 v, (R_0 H U_0 / \ell) w, \rho_* f_0 U_0 \ell \psi, (\rho_* f_0 U_0 \ell / g H) \rho],$$

where $R_0 = U_0 / f_0 \ell$ is the Rossby number, ρ_* is a constant reference density, and the other quantities are defined in (2.3).

Like MM we seek solutions of (2.5) - (2.8) of the form

$$\psi = \bar{\psi} + \psi', \quad (2.11)$$

where

$$\bar{\psi}(y, z, t) = \lim_{L \rightarrow \infty} \frac{1}{2L} \int_{-L}^L \psi dx \quad (2.12)$$

represents a wave-induced mean field which yields the mean current $\bar{u} = -\bar{\psi}_y$ parallel to the barrier, and ψ' represents a fluctuating field which consists of the superposition of the incident and reflected waves. Upon substituting (2.11) into (2.5) we obtain

$$\partial_t [\bar{\psi}_{yy} + (B^{-1} \bar{\psi}_z)_z] + \beta^* \sin \alpha \bar{\psi}_y + R^* \bar{\psi}_{yy} - A^* \bar{\psi}_{yyyy} = M_{yy} - H_{yz}, \quad (2.13)$$

where

$$M = -\overline{\psi_y' \psi_x'} = \overline{u' v'}, \quad (2.14)$$

and

$$H = \overline{\psi_x' B^{-1} \psi_z'} = \overline{v' B^{-1} (-\rho')}. \quad (2.15)$$

Performing the same operations on the boundary conditions (2.6) to (2.8), we find

$$\bar{\psi} = 0 \quad \text{at} \quad y = 0 \quad (2.16)$$

$$\bar{\psi}_{zt} + \frac{\partial}{\partial y} (\bar{\psi}_x \bar{\psi}_z') = 0 \quad \text{at} \quad z = 0, -1 \quad (2.17)$$

$$\bar{\psi}_y = 0 \quad \text{at} \quad y = 0 \quad (2.18)$$

We assume that the fluctuations under consideration satisfy a linearized version of (2.5), which, in dimensional form, reads

$$\nabla^2 \psi_t' + \left(\frac{f_0^2}{N^2} \psi_{zt}' \right)_z + \beta (\sin \alpha \psi_y' + \cos \alpha \psi_x') = -R \nabla^2 \psi' + A \nabla^2 (\nabla^2 \psi') \quad (2.19)$$

with boundary conditions

$$\psi' = 0 \quad \text{at} \quad y = 0 \quad (2.20)$$

$$\psi_z' = 0 \quad \text{at} \quad z = 0, -H \quad (2.21)$$

$$\psi_y' = 0 \quad \text{at} \quad y = 0, \quad (2.22)$$

$$\psi' \text{ finite as } y \rightarrow \infty \quad (2.23)$$

Equation (2.19) has four approximate solutions: the observed incoming wave,

$$\psi_{in} = \psi_I(z) e^{i(k_1 x + k_2 y - \omega t)} \quad (2.24)$$

with real wave numbers k_1, k_2 ; the reflected wave,

$$\psi_{re} = \psi_I(z) e^{i(\ell_1 x + \ell_2 y - \omega t)} \quad (2.25)$$

where $\ell_1 = k_1$ and $\ell_2 = \ell_{2r} + i \ell_{2i}$

and ℓ_{2r}, ℓ_{2i} are given as in MM (A9, A10); and two solutions of

$$\psi_{t yy}' = -R \psi_{yy}' + A \psi_{yyyy}' \quad (2.26)$$

$$\psi' = \psi_I(z) e^{i(m_1 x \pm m_2 y - \omega t)} \quad (2.27)$$

where $m_1 = k_1$ and

$$m_2 = \frac{\omega}{\sqrt{2A}} [R + (R^2 + \omega^2)^{1/2}]^{-1/2} + i \frac{1}{\sqrt{2A}} [R + (R^2 + \omega^2)^{1/2}]^{1/2} \quad (2.28)$$

Considering (2.23), we find that our total wave field is the real part of

$$\psi' = \psi_I(z) (e^{ik_2 y} + \alpha_1 e^{i\ell_2 y} + \alpha_2 e^{im_2 y}) e^{i(k_1 x - \omega t)}, \quad (2.29)$$

where α_1, α_2 are complex constants to be determined by the boundary conditions (2.20) and (2.22). For $A = 0$ (as in MM) we would get $\alpha_1 = -1$ and $\alpha_2 = 0$. In the general case ($A \neq 0$) we obtain

$$\alpha_1 = \frac{m_2 - k_2}{\ell_2 - m_2}, \quad \alpha_2 = \frac{k_2 - \ell_2}{\ell_2 - m_2}. \quad (2.30)$$

Substituting the real part of (2.29) into (2.14) and (2.15) yields

$$M = -\frac{1}{2} \psi_I^2(z) k_1 \left\{ k_2 + \alpha_1 \alpha_1^* \ell_{2r} e^{-2\ell_2 i y} + \alpha_2 \alpha_2^* m_{2r} e^{-2m_2 i y} + B e^{-\ell_2 i y} + C e^{-m_2 i y} + D e^{-(\ell_2 i + m_2 i) y} \right\}, \quad (2.31)$$

where

$$B = \text{Re}[\alpha_1(k_2 + \ell_2)] \cos[(k_2 - \ell_{2r})y] + \text{Im}[\alpha_1(k_2 + \ell_2)] \sin[(k_2 - \ell_{2r})y], \quad (2.32)$$

$$C = \text{Re}[\alpha_2(k_2 + m_2)] \cos[(k_2 - m_{2r})y] + \text{Im}[\alpha_2(k_2 + m_2)] \sin[(k_2 - m_{2r})y], \quad (2.33)$$

$$D = \text{Re}[\alpha_1 \alpha_2^* \ell_2 + \alpha_1^* \alpha_2 m_2] \cos[(\ell_{2r} - m_{2r})y] + \text{Im}[-\alpha_1 \alpha_2^* \ell_2 + \alpha_1^* \alpha_2 m_2] \sin[(\ell_{2r} - m_{2r})y], \quad (2.34)$$

and

$$H = 0. \quad (2.35)$$

From (2.31) on, a superscript asterisk denotes the complex conjugate.

At this point we note that, if we had introduced an average with respect to time instead of (2.12), we would have obtained exactly the same expressions for M and H .

As M and H are independent of t we can find a steady solution $\bar{\psi}_s$ of (2.13). The boundary current (Eulerian mean flow) $\bar{u}_s = -\bar{\psi}_y$ will then have to satisfy the (dimensional) equation

$$A \frac{d^3 \bar{u}_s}{dy^3} - R \frac{d \bar{u}_s}{dy} - \beta \sin \alpha \bar{u}_s = - \frac{P_I^2(z)}{\rho_*^2 f_0^2} G(y), \quad (2.36)$$

where

$$G(y) = \frac{-M_{yy}}{\psi_I^2(z)}, \quad (2.37)$$

and $P_I(z)$ is the amplitude of the pressure fluctuation associated with the incoming Rossby wave.

As boundary conditions we choose

$$u_s = 0 \quad \text{at } y = 0, \quad (2.38)$$

$$u_s \rightarrow 0 \quad \text{as } y \rightarrow \infty, \quad (2.39)$$

and

$$\int_0^\infty \bar{u}_s dy = 0. \quad (2.40)$$

Equation (2.40) implies that there is no flow around the ridge as $x \rightarrow \pm \infty$. MM also used the nonslip condition (2.38) although, based on the Rayleigh damping, there was no physical reason for using this condition. MM should have used (2.40) instead. It is fortunate that, for the MM solution, (2.38) and (2.40) are numerically equivalent.

The solution of (2.36) and (2.38) - (2.40) is

$$\bar{u}_s(y, z) = \frac{P_I^2(z) k_1}{2A \rho_*^2 f_0^2} \left[[K(0)(\cos y + \frac{\sigma}{\tau} \sin y) + \frac{(\sigma^2 + \tau^2) \sin y}{\tau} \int_0^\infty K(y) dy] - K(y) \right] \quad (2.41)$$

where

$$K(y) = \frac{2}{k_1} e^{\gamma_1 y} \int_{+\infty}^y e^{(\gamma_2 - \gamma_1) y'''} \frac{y'''}{f} e^{(\gamma_3 - \gamma_2) y''} \int_{+\infty}^{y''} e^{-\gamma_3 y'} G(y') dy' dy'' dy''', \quad (2.42)$$

$$\sigma = -\frac{1}{2}(r_1 + r_2), \quad \tau = \frac{\sqrt{3}}{2}(r_1 - r_2), \quad \gamma_1 = (r_1 + r_2),$$

$$\gamma_2, \gamma_3 = -\frac{1}{2}(r_1 + r_2) \pm i \frac{\sqrt{3}}{2}(r_1 + r_2),$$

and

$$r_1, r_2 = \left[\frac{\beta \sin \alpha}{2A} \pm \left(\frac{\beta^2 \sin^2 \alpha}{4A^2} - \frac{R^3}{27A^3} \right)^{1/2} \right]^{1/3}.$$

Generalization to the case of a random incident Rossby wave field, whose potential energy spectrum is known, is done as in MM and leads to

$$\bar{u}_s(y, z) = \frac{\tilde{p}_I^2(z)}{A \rho_*^2 f_0^2 r^2} \int_{v_1}^{v_2} k_1 E_{\text{pot}}(v) \left\{ [K(0, v)(\cos y + \frac{\sigma}{\tau} \sin y) + \frac{(\sigma^2 + \tau^2) \sin y}{\tau} \int_0^\infty K(y, v) dy] - K(y, v) \right\} dv, \quad (2.43)$$

where k_1, k_2, l_2, m_2 are functions of the cyclic frequency $v = \omega/2\pi$,

$K(y, v)$ is defined as in (2.42) where k_1 and G are now functions of also, $E_{\text{pot}}(v)$ is the potential energy spectrum of the incoming (observed) Rossby wave field, $\tilde{p}_I(z)$ is the normalized (as in MM) first

pressure mode, and $r = \frac{d\tilde{p}_I/dz}{N^2 \tilde{\zeta}_I}$, where $\tilde{\zeta}_I$ describes the normalized (as in

MM) vertical distribution of the first-mode particle displacements.

Figure 1 shows the horizontal distribution of the surface Eulerian mean flow $\bar{u}_s(y, 0)$, according to (2.43), for the case of the observed incoming

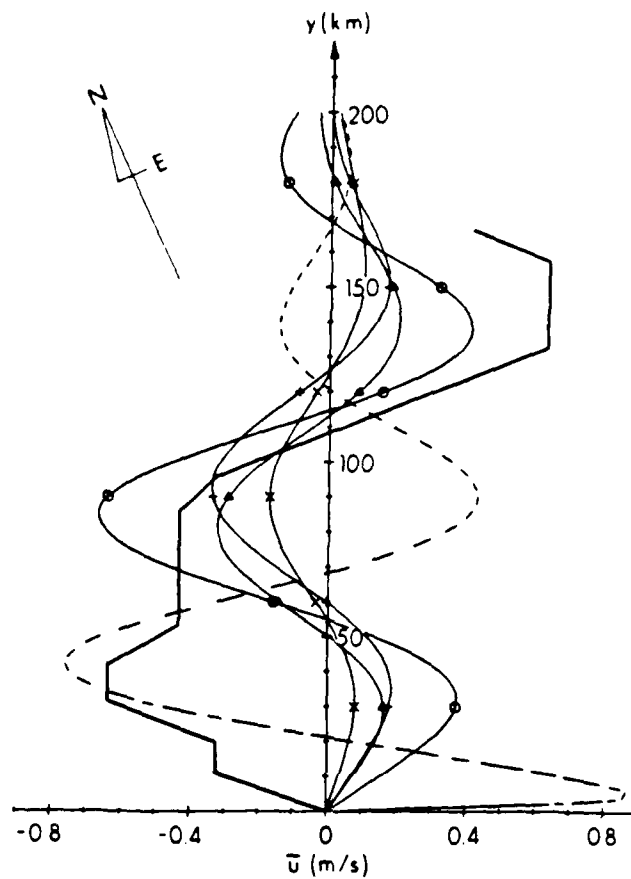


Fig. 1. The horizontal distribution of the surface Eulerian mean flow along the north side of the Hawaiian Ridge.

full line	observed	(after White, 1983, extrapolating his 100/400 db values to 0/1000 db values on the basis of the depth distribution shown in Fig. 3 of MM)
broken line	$A = 0$	$R = 5 \times 10^{-8} s^{-1}$ (from MM)
circles	$A = 1 \times 10^2 m^2 s^{-1};$	$R = 1 \times 10^{-8} s^{-1}$
triangles	$A = 1 \times 10^2 m^2 s^{-1};$	$R = 5 \times 10^{-8} s^{-1}$
crosses (+)	$A = 2 \times 10^2 m^2 s^{-1};$	$R = 1 \times 10^{-8} s^{-1}$
crosses (x)	$A = 2 \times 10^2 m^2 s^{-1};$	$R = 5 \times 10^{-8} s^{-1}$

baroclinic Rossby wave field as described in MM. Except for R and A all numerical values of the various parameters are as in MM. This figure shows the current for four different combinations of R and A. For comparison the result of MM (i.e. A = 0) and the observed current (White, 1983) are also given. The vertical distribution of the mean flow is as in Figure 3 of MM.

3. THE LAGRANGIAN MEAN FLOW

According to Longuet-Higgins (1969) the x-component of the Stokes drift associated with a single wave is

$$\bar{u}_{st} = \left[\int_{t_0}^t \underline{u}' dt' \right] \cdot \nabla u' , \quad (3.1)$$

where \underline{u}' is the wave-associated velocity vector, and the overbar denotes a time average over one or more wave cycles. For a wave field containing waves of various periods we replace (3.1) by

$$\bar{u}_{st} = \lim_{T \rightarrow \infty} \frac{1}{T} \int_{t_0}^{t_0+T} \left[\int_{t_0}^{t'} \underline{u}' dt' \right] \cdot \nabla u' dt . \quad (3.2)$$

Using (3.1) we obtain for a single pair of incoming and reflected Rossby waves (in nondimensional form)

$$\bar{u}_{st} = \frac{k_1 \psi_I^2(z)}{2\omega} Q(y) , \quad (3.3)$$

where

$$Q(y) = 2\alpha_1 \alpha_1^* \ell_{2i}^2 e^{-2\ell_{2i}y} + 2\alpha_2 \alpha_2^* m_{2i} e^{-2m_{2i}y} + B'e^{-\ell_{2i}y} + C'e^{-m_{2i}y} + D'e^{-(\ell_{2i} + m_{2i})y} , \quad (3.4)$$

where

$$B' = \text{Re} [-\alpha_1 (k_2 - \ell_2)^2] \cos[(k_2 - \ell_{2r})y] + \text{Im} [-\alpha_1 (k_2 - \ell_2)^2] \sin[(k_2 - \ell_{2r})y] , \quad (3.5)$$

$$C' = \text{Re} [-\alpha_2 (k_2 - m_2)^2] \cos[(k_2 - m_{2r})y] + \text{Im} [-\alpha_2 (k_2 - m_2)^2] \sin[(k_2 - m_{2r})y] , \quad (3.6)$$

and

$$D' = \text{Re}[2\alpha_1\alpha_2^*(\alpha_2m_2)^* - \alpha_1^*\alpha_2m_2^2 - \alpha_1\alpha_2^*\alpha_2^2] \cos[(\alpha_{2R} - m_{2R})y] \\ + \text{Im}[-2\alpha_1\alpha_2^*(\alpha_2m_2)^* - \alpha_1^*\alpha_2m_2^2 + \alpha_1\alpha_2^*\alpha_2^2] \sin[(\alpha_{2R} - m_{2R})y] \quad (3.7)$$

The y-component, \bar{v}_{st} , of the Stokes drift vanishes.

For the case of a random wave field we obtain (in dimensional form)

$$\bar{u}_{st}(y,z) = \frac{\bar{p}_1^2(z)}{c_*^2 f_0^2 r^2} \int_{v_1}^{v_2} \frac{k_1}{\omega} E_{pot}(v) Q(y,v) dv \quad (3.8)$$

Figure 2 shows the horizontal distribution of the surface Stokes drift $\bar{u}_{st}(y,0)$ according to (3.8), for the same numerical values as used for the Eulerian mean flow, which is also displayed for comparison. In addition, it shows the Lagrangian mean flow

$$\bar{u}_L = \bar{u}_s + \bar{u}_{st} \quad (3.9)$$

4. DISCUSSION

Compared to the case of vanishing lateral friction (MM, Figure 4), in the case of $A \neq 0$ (Figure 1) the current speed is smaller and the width of the current bands is larger. The narrow eastward jet in the immediate neighborhood of the Ridge, as shown in MM (for $A = 0$), is replaced by a much weaker, broader eastward flow. The subsequent western current, which we would still call a western boundary current, reaches a strength similar to that in MM only if values for R are decreased. Because of the broader eastward current directly along the Ridge, the western boundary current and the subsequent eastward countercurrent are now shifted farther away from the Ridge. This means a better agreement with White's (1983) observation which is also indicated in Figure 1.

The significance of the comparison of our theoretical predictions with White's observational results should not be overestimated. White's results rest on a thin data base. In addition, even if theory and observations were perfect, one should not expect perfect agreement between them. The reflection of Rossby waves is not the only potential driving mechanism of a mean flow along the Hawaiian Ridge; in addition, there can be a wind-driven flow which is not included in our present theory. What our theory does predict is a mean current system north of the Hawaiian Ridge that is entirely driven by baroclinic Rossby waves and that has a significant magnitude. Remarkably enough, this system shows a resemblance with an observed current system. We conclude that the role of the Rossby waves in the generation process of this current system is significant.

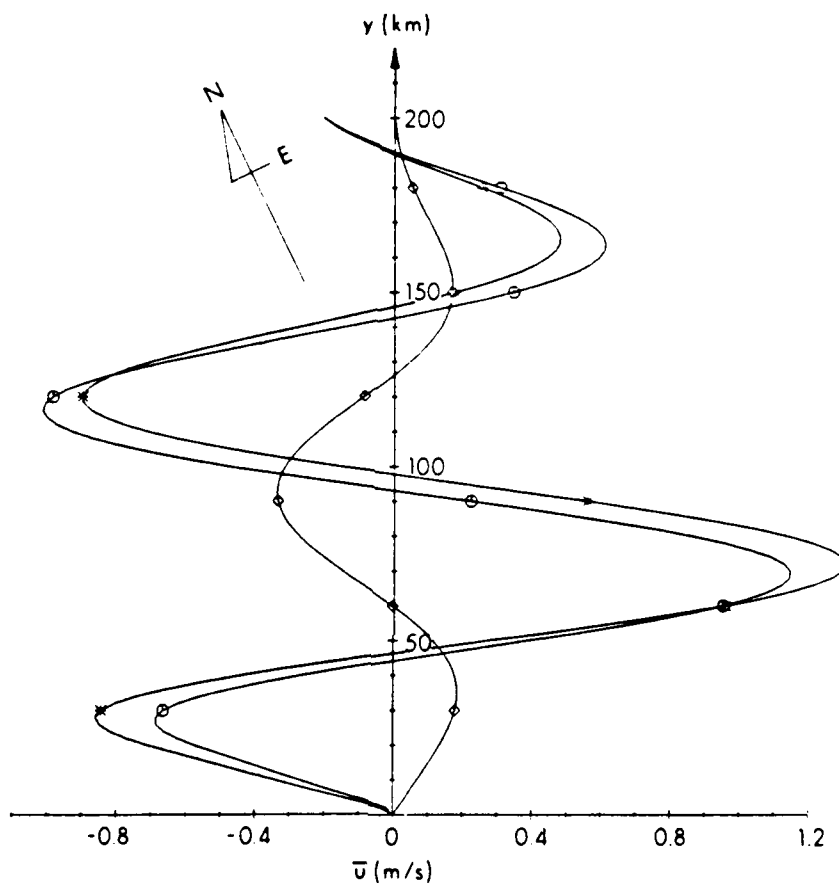


Fig. 2. The horizontal distribution of surface mean flows along the north side of the Hawaiian Ridge. The numerical values for the friction parameters are $A = 2 \times 10^2 \text{ m}^2 \text{ s}^{-1}$ and $R = 1 \times 10^{-8} \text{ s}^{-1}$.

rhombi	Eulerian mean flow
asterisks	Stokes drift
circles	Lagrangian mean flow

Table 1. Maximum values of current speed (in ms^{-1}) for the first three bands of the Eulerian mean flow for various combinations of R and A values.

R (10^{-8}s^{-1})	A ($10^2\text{m}^2\text{s}^{-1}$)	Eastward Coastal flow	Westward Boundary flow	Eastward Counter flow
1.0	0.5	0.647	1.139	0.822
1.0	1.0	0.374	0.663	0.408
1.0	2.0	0.184	0.338	0.167
1.0	5.0	0.057	0.117	0.044
1.0	10.0	0.019	0.050	0.015
2.5	0.5	0.465	0.854	0.587
2.5	1.0	0.266	0.503	0.308
2.5	2.0	0.131	0.256	0.135
2.5	5.0	0.040	0.092	0.039
2.5	10.0	0.013	0.041	0.015
5.0	0.5	0.287	0.538	0.354
5.0	1.0	0.163	0.323	0.200
5.0	2.0	0.080	0.170	0.097
5.0	5.0	0.024	0.063	0.032
5.0	10.0	0.008	0.029	0.014

Table 2. ϵ - Rossby numbers (ϵ) for reflected Rossby waves for various R, A combinations.

R (10^{-8}s^{-1})	A ($10^2\text{m}^2\text{s}^{-1}$)	ϵ (at 6.7 - year peak)	ϵ (for annual waves)
1	0.5	122	4 - 60
1	1.0	89	4 - 50
1	2.0	66	4 - 37
1	5.0	47	3 - 25
1	10.0	38	2 - 19
5	0.5	11	4 - 53
5	1.0	8	4 - 44
5	2.0	5	4 - 32
5	5.0	3	3 - 21
5	10.0	3	2 - 16

The Lagrangian mean flow associated with the Rossby waves is mainly dominated by the Stokes drift (Figure 2). Over the first 100 km off the Ridge the Stokes drift more than offsets the Eulerian mean flow such that the Eulerian and Lagrangian mean flows are mostly in opposite directions, and the Lagrangian flow is stronger than the Eulerian.

The introduction of lateral friction allows meaningful mean flows even when the Rayleigh damping coefficient is small ($R = 1 \times 10^{-8} \text{s}^{-1}$). Figure 1 shows the Eulerian mean flow for four combinations of R and A. Maximum current speeds for a larger number of R, A combinations are found in Table 1. $R = 1 \times 10^{-8} \text{s}^{-1}$ means a relaxation time of 1000 days, i.e. annual waves do not lose their wave nature through Rayleigh damping as they did (more or less) in MM, where $R = 5 \times 10^{-8} \text{s}^{-1}$ was chosen.

As another test of the wave nature of our "wave" solutions we have

calculated the corresponding β -Rossby number $\epsilon = \frac{2Uk^2}{\beta}$, where $k = \frac{2\pi}{\lambda}$

and λ is the wave length and U is the scale of the particle velocity. For the incoming waves, $\epsilon = 2 \times 10^{-2}$ at the 6.7-year peak, and ϵ -values for the broad annual peak range from 0.1 to 1.4 and most values are smaller than one. Clearly, these waves can propagate as free waves. For the reflected waves, ϵ -values are largest near the barrier. Table 2 shows their ϵ -values at the 6.7-year peak and for the annual peak for various R, A combinations. Naturally the influence of R on ϵ is stronger at the 6.7-year period than for the annual waves. At the 6.7-year period the reflected wave cannot propagate as a free wave because it is damped too strongly either by Rayleigh damping or by nonlinear effects. For the annual waves the influence of R is smaller. For $R = 1 \times 10^{-8} \text{s}^{-1}$, Rayleigh damping does not eliminate the reflected annual wave's possibility of propagating as waves; ϵ -values of 2 to about 50, however, make the applicability of linear theory to our problem at least a controversial issue.

We have tried to include nonlinear effects, especially the action of the mean flow on the reflected waves, in our analytical study; however, the technical difficulties associated with such an attempt appeared insurmountable. We are taking the point of view that we cannot go beyond our present study by means of analytical tools. We are planning to continue this work by means of numerical methods.

ACKNOWLEDGMENTS

We would like to thank J. Willebrand for helpful discussions of this manuscript. This research has been supported by the office of Naval Research whose support is gratefully acknowledged. This is Hawaii Institute of Geophysics Report HIG-84-1.

REFERENCES

- Longuet-Higgins, M. S., 1969: On the transport of mass by time-varying ocean currents. Deep Sea Res., 16, 431 - 477.
- Magaard, L., 1983: On the potential energy of baroclinic Rossby waves in the North Pacific. J. Phys. Oceanogr., 13, 38 - 42.
- Mysak, L. A. and L. Magaard, 1983: Rossby wave driven Eulerian mean flows along non-zonal barriers, with application to the Hawaiian Ridge. J. Phys. Oceanogr., 13, 1716 - 1725.
- White, W. B., 1983: A narrow boundary current along the eastern side of the Hawaiian Ridge; the North Hawaiian Ridge Current. J. Phys. Oceanogr., 13, 1726 - 1731.

Unclassified

SECURITY CLASSIFICATION OF THIS PAGE (When Data Entered)

REPORT DOCUMENTATION PAGE		READ INSTRUCTIONS BEFORE COMPLETING FORM
1. REPORT NUMBER HIG 84-1	2. GOVT ACCESSION NO. AD A144 957	3. RECIPIENT'S CATALOG NUMBER
4. TITLE (and Subtitle) An Improved Analytical Theory of Rossby Wave Driven Eulerian and Lagrangian Mean Flows Along Non-Zonal Barriers, With Application to the Hawaiian Ridge		5. TYPE OF REPORT & PERIOD COVERED
7. AUTHOR(s) Im Sang Oh and Lorenz Magaard		6. PERFORMING ORG. REPORT NUMBER HIG Technical Report 84-1
9. PERFORMING ORGANIZATION NAME AND ADDRESS Hawaii Institute of Geophysics 2525 Correa Road Honolulu, Hawaii 96822		8. CONTRACT OR GRANT NUMBER(s) N00014-82-C-0380
11. CONTROLLING OFFICE NAME AND ADDRESS Office of Naval Research Ocean Sciences and Technology Division Bay St. Louis, MS 39520		10. PROGRAM ELEMENT PROJECT, TASK AREA & WORK UNIT NUMBERS Analytical Modelling
14. MONITORING AGENCY NAME & ADDRESS (if different from Controlling Office) Office of Naval Research Branch Office 1030 East Green Street Pasadena, CA 91106		12. REPORT DATE May 1984
		13. NUMBER OF PAGES 17
		15. SECURITY CLASS. (of this report) Unclassified
		15a. DECLASSIFICATION/DOWNGRADING SCHEDULE
16. DISTRIBUTION STATEMENT (of this Report) Approved for public release; distribution unlimited.		
17. DISTRIBUTION STATEMENT (of the abstract entered in Block 20, if different from Report)		
18. SUPPLEMENTARY NOTES Published as Hawaii Institute of Geophysics Technical Report 84-1		
19. KEY WORDS (Continue on reverse side if necessary and identify by block number) Rossby Wave Non-Zonal Barrier Eulerian Mean Flow Hawaiian Ridge Langrangian Mean Flow Wave Reflection		
20. ABSTRACT (Continue on reverse side if necessary and identify by block number) We study the reflection of baroclinic Rossby waves from a non-zonal barrier. In doing so we improve and extend an analytical study by Mysak and Magaard (1983). We add lateral friction to their model and obtain not only a more realistic Eulerian secondary flow, but we also calculate the Stokes drift of the total Rossby wave field. We apply our improved and extended model to the Hawaiian Ridge where the incident wave field is known (Magaard, 1983). (over)		

DD FORM 1473
1 JAN 73

EDITION OF 1 NOV 65 IS OBSOLETE
S/N 0102-014-6601

Unclassified
SECURITY CLASSIFICATION OF THIS PAGE (When Data Entered)

Unclassified

SECURITY CLASSIFICATION OF THIS PAGE(When Data Entered)

Compared to the case of vanishing lateral friction the Eulerian mean flow now shows smaller current speeds and wider current bands. The narrow eastward jet in the immediate neighborhood of the Ridge is now replaced by a much weaker, broader eastward flow. The subsequent western boundary current and eastward countercurrent are now shifted farther away from the Ridge in better agreement with White's (1983) analysis of historical temperature data. The Lagrangian mean flow is stronger than the Eulerian mean flow. Within the first 100 km off the Ridge the two flows are mostly in opposite directions.

Unclassified

SECURITY CLASSIFICATION OF THIS PAGE(When Data Entered)

**LATE
LME**